

Spontaneously Resolved Homochiral 3D Lanthanide–Silver Heterometallic Coordination Framework with Extended Helical Ln–O–Ag Subunits

Xiaojun Gu and Dongfeng Xue*

State Key Laboratory of Fine Chemicals, Department of Materials Science and Chemical Engineering, School of Chemical Engineering, Dalian University of Technology, Dalian 116012, People's Republic of China

Received May 11, 2006

Two novel homochiral lanthanide–silver heterometallic coordination polymers LnAg(OAc)(IN)₃ [Ln = Nd (**1**), Eu (**2**), HIN = isonicotinic acid, HOAc = acetic acid] have been prepared under hydrothermal conditions, which were characterized by elemental analysis, infrared, thermogravimetric analysis, and single-crystal X-ray diffraction. Both complexes are isostructural and crystallize in a hexagonal system, chiral space group *P6₃22*. Both polymers are constructed from infinite right-handed homochiral helical chains with Ln–O–Ag connectivity, representing the first examples of homochiral lanthanide–transition metal heterometallic coordination polymers with a 3D coordination framework based on spontaneous resolution. Furthermore, the luminescent properties of **2** were studied.

Introduction

The design of chiral metal–organic coordination polymers has attracted much attention not only because of their potential applications in enantioselective separation, nonlinear optical, and magnetic properties but also because of their intriguing architectures.^{1–4} To date, two general approaches have been adopted for the synthesis of such materials: (i) enantioselective synthesis using chiral species, which yields enantiopure products, and (ii) spontaneous resolution upon crystallization without any chiral auxiliary, generating a conglomerate. By the first approach, many homochiral coordination polymers have been obtained.^{5,6} In contrast, homochiral coordination polymers generated by the second

method are still rare because their mechanism remains poorly understood.⁴ There are only a few examples of spontaneous resolution, where the chiral information in the building units can be transmitted into higher dimensionality to generate homochiral coordination polymers.^{4,7} However, almost all of these reported homochiral coordination polymers have been attributed to a homometallic system, while the chemistry toward homochiral lanthanide–transition metal (Ln–M) heterometallic coordination polymers based on spontaneous resolution remains largely unexplored.

Recently, high-dimensional Ln–M heterometallic coordination polymers have attracted increasing attention because of their interesting structural topologies and the significance

* To whom correspondence should be addressed. E-mail: dfxue@chem.dlut.edu.cn. Tel/Fax: +86-411-88993623.

- (1) (a) Pérez-García, L.; Amabilino, D. B. *Chem. Soc. Rev.* **2002**, *31*, 342. (b) Moulton, B.; Zaworotko, M. J. *Chem. Rev.* **2001**, *101*, 1629. (c) Kesaneli, B.; Lin, W. *Coord. Chem. Rev.* **2003**, *246*, 305. (d) Bradshaw, D.; Claridge, J. B.; Cussen, E. J.; Prior, T. J.; Rosseinsky, M. J. *Acc. Chem. Res.* **2005**, *38*, 273. (e) Rao, C. N. R.; Natarajan, S.; Vaidhyanathan, R. *Angew. Chem., Int. Ed.* **2004**, *43*, 1466.
- (2) Seo, J. S.; Whang, D.; Lee, H.; Jun, S. I.; Oh, J.; Jeon, Y. J.; Kim, K. *Nature (London)* **2000**, *404*, 982.
- (3) (a) Kepert, C. J.; Prior, T. J.; Rosseinsky, M. J. *J. Am. Chem. Soc.* **2000**, *122*, 5158. (b) Bradshaw, D.; Prior, T. J.; Cussen, E. J.; Claridge, J. B.; Rosseinsky, M. J. *J. Am. Chem. Soc.* **2004**, *126*, 6106.
- (4) (a) Maggard, P. A.; Stern, C. L.; Poeppelmeier, K. R. *J. Am. Chem. Soc.* **2001**, *123*, 7742. (b) Katsuki, I.; Motoda, Y.; Sunatsuki, Y.; Matsumoto, N.; Nakashima, T.; Kojima, M. *J. Am. Chem. Soc.* **2002**, *124*, 629. (c) Gao, E. Q.; Yue, Y. F.; Bai, S. Q.; He, Z.; Yan, C. H. *J. Am. Chem. Soc.* **2004**, *126*, 1419.

- (5) (a) Cui, Y.; Lee, S. J.; Lin, W. *J. Am. Chem. Soc.* **2003**, *125*, 6014. (b) Wu, C. D.; Hu, A.; Zhang, L.; Lin, W. *J. Am. Chem. Soc.* **2005**, *127*, 8940.
- (6) (a) Xiong, R. G.; You, X. Z.; Abrahams, B. F.; Xue, Z.; Che, C. M. *Angew. Chem., Int. Ed.* **2001**, *40*, 4422. (b) Shi, X.; Zhu, G. S.; Qiu, S. L.; Huang, K. L.; Yu, J. H.; Xu, R. R. *Angew. Chem., Int. Ed.* **2004**, *43*, 6482. (c) Anokhina, E. V.; Jacobson, A. J. *J. Am. Chem. Soc.* **2004**, *126*, 3044.
- (7) (a) Tabellion, F. M.; Seidel, S. R.; Arif, A. M.; Stang, P. J. *Angew. Chem., Int. Ed.* **2001**, *40*, 1529. (b) Sasa, M.; Tanaka, K.; Bu, X. H.; Shiro, M.; Shionoya, M. *J. Am. Chem. Soc.* **2001**, *123*, 10750. (c) Siemeling, U.; Scheppelman, I.; Neumann, B.; Stammer, A.; Stammer, H.-G.; Frelek, J. *Chem. Commun.* **2003**, 2236. (d) Wang, Y. T.; Tong, M. L.; Fan, H. H.; Wang, H. Z.; Chen, X. M. *Dalton Trans.* **2005**, 424. (e) Biradha, K.; Seward, C.; Zaworotko, M. J. *Angew. Chem., Int. Ed.* **1999**, *38*, 492. (f) Vaidhyanathan, R.; Natarajan, S.; Rao, C. N. R. *J. Solid State Chem.* **2004**, *177*, 1444.

of discovering new materials.^{8,9} However, because of complicated interactions among the organic moiety and two types of metal centers, the construction of a homochiral Ln–M heterometallic coordination framework is one of the most challenging issues in synthetic chemistry and materials science. Fortunately, the characteristic of lanthanide and transition-metal ions with different affinities for O and N donors might provide the impetus for homochiral discriminative interactions between two chiral components. Inspired by the aforementioned considerations, we have attempted to study the systematic synthesis of homochiral Ln–M heterometallic coordination polymers. In the current work, we choose isonicotinic acid (IN) with both N and O donor atoms as a linker between the lanthanide and transition-metal ions because this rigid ligand has been proven to be able to form novel structures with 3D Ln–M heterometallic coordination frameworks.⁹ Here, we report two novel homochiral 3D Ln–M coordination polymers LnAg(OAc)(IN)₃ [Ln = Nd (**1**), Eu (**2**), HOAc = acetic acid] containing right-handed helical chains with Ln–O–Ag connectivity.

Experimental Section

Materials. All chemicals purchased were of reagent grade and were used without further purification. Water used in all reactions was distilled water.

Physical Measurements. The elemental analyses (C, H, and N) were carried out a Perkin-Elmer 240C elemental analyzer; Nd, Eu, and Ag were analyzed on a PLASMA-SPEC(I) inductively coupled plasma atomic emission spectrometer. The infrared (IR) spectra were recorded (400–4000 cm⁻¹ region) on an Alpha Centaurt Fourier transform IR spectrophotometer using KBr pellets. Thermogravimetric analyses (TGA) were performed on an SDT Q600 instrument in a flowing N₂ atmosphere with a heating rate of 10 °C/min. Fluorescence spectroscopy data were recorded on a SPEX FL-2T2 luminescence spectrometer equipped with a 450-W Xe lamp as the excitation source.

Synthesis of [NdAg(OAc)(IN)₃] (1**).** A mixture of Nd₂O₃ (0.168 g, 0.5 mmol), AgNO₃ (0.034 g, 0.2 mmol), HIN (0.123 g, 1.0 mmol), HOAc (0.030 g, 0.5 mmol), and water (8 mL) was sealed in a 23-mL Teflon reactor and was kept under autogenous pressure at 180 °C for 4 days. Pink octahedron-shaped crystals were filtered off, washed with distilled water, and dried in air (yield: 0.061 g, 45% based on Ag). The as-synthesized material is insoluble in water and common organic solvents. Elem anal. Calcd for C₂₀H₁₅AgN₃NdO₈: Nd, 21.29; Ag, 15.92; C, 35.42; H, 2.21; N, 6.20. Found: Nd, 21.21; Ag, 15.97; C, 35.59; H, 2.27; N, 6.14. IR (KBr pellet, cm⁻¹): 3470(w), 3045(w), 3029(w), 1635(m), 1595(s), 1537(s), 1459(w), 1406(s), 1225(w), 1059(w), 1001(w), 951(w), 853(w), 766(m), 680(m), 601(w), 548(w).

Table 1. Crystal Data and Structure Refinement for Compounds **1** and **2**

compound	1	2
empirical formula	C ₂₀ H ₁₅ AgN ₃ NdO ₈	C ₂₀ H ₁₅ AgN ₃ EuO ₈
fw	677.46	685.18
temp (K)	293(2)	293(2)
cryst syst	hexagonal	hexagonal
space group	P6 ₁ 22	P6 ₁ 22
a (Å)	11.8241(8)	11.8098(6)
c (Å)	27.418(3)	27.279(3)
V (Å ³)	3319.8(5)	3294.9(4)
Z	6	6
ρ _{calcd} (g cm ⁻³)	2.033	2.072
μ (mm ⁻¹)	3.257	3.773
F(000)	1962	1980
GOF	1.024	1.026
R _{int}	0.0705	0.0671
R1 ^a [I > 2σ(I)]	0.0323	0.0308
wR2 ^b [I > 2σ(I)]	0.0568	0.0515

$$^a R1 = \sum ||F_o| - |F_c|| / \sum |F_o|. \quad ^b wR2 = \sum [w(F_o^2 - F_c^2)^2] / \sum [w(F_o^2)^2]^{1/2}.$$

Synthesis of [EuAg(OAc)(IN)₃] (2**).** A procedure identical with that of **1** was followed to prepare **2** except that Nd₂O₃ was replaced by Eu₂O₃ (0.176 g, 0.5 mmol). Colorless octahedron-shaped crystals were obtained (yield: 0.067 g, 49% based on Ag). Elem anal. Calcd for C₂₀H₁₅AgN₃EuO₈: Eu, 22.19; Ag, 15.74; C, 35.04; H, 2.19; N, 6.13. Found: Eu, 22.15; Ag, 15.79; C, 35.16; H, 2.12; N, 6.05. IR (KBr pellet, cm⁻¹): 3436(w), 3068(w), 3029(w), 1639(m), 1598(s), 1540(s), 1461(w), 1407(s), 1226(w), 1054(w), 1003(w), 949(w), 853(w), 766(m), 689(m), 602(w), 543(w).

X-ray Crystallographic Study. The collection of crystallographic data was carried out on a Bruker SMART Apex CCD diffractometer using graphite-monochromated Mo Kα radiation (λ = 0.710 73 Å) at 293 K. Empirical absorption correction was applied. The structures were solved by direct methods and refined by full-matrix least-squares methods on F² using the *SHELXTL* crystallographic software package.¹⁰ Anisotropic thermal parameters were used to refine all non-H atoms. The H atoms for C–H were placed in idealized positions. The Flack parameters of +0.00(2) and -0.024(15) for **1** and **2**, respectively, indicate that the absolute configurations are correct. The crystal data and structure refinement of compounds **1** and **2** are summarized in Table 1. Selected bond lengths and angles for compounds **1** and **2** are listed in Table 2.

Results and Discussion

Single-crystal X-ray diffraction analyses reveal that **1** and **2** crystallize in the high-symmetry hexagonal space group P6₁22 and possess a homochiral 3D heterometallic coordination framework constructed from inorganic right-handed helical chains and IN linkers. Because **1** and **2** are isostructural, only the structure of **1** is described in detail. An ORTEP view of **1** is shown in Figure 1. There are half of Nd(III) ions, half of Ag(I) ions, half of OAc, and one and half crystallographically unique IN ligands in the asymmetrical unit. Each Ag(I) ion is four-coordinated via two O atoms from two OAc ligands [Ag–O 2.327(3) Å] and two N atoms from two bridging IN ligands [Ag–N 2.309(4) Å] to furnish a tetrahedral geometry. The Nd(III) ion displays a bicapped trigonal prism geometry coordinated by two O atoms from

- (8) (a) Cutland-Van Noord, A. D.; Kampf, J. W.; Pecoraro, V. L. *Angew. Chem., Int. Ed.* **2002**, *41*, 4668. (b) Zhou, Y. F.; Jiang, F. L.; Yuan, D. Q.; Wu, B. L.; Wang, R. H.; Lin, Z. Z.; Hong, M. C. *Angew. Chem., Int. Ed.* **2004**, *43*, 5665. (c) Zhao, B.; Chen, X. Y.; Cheng, P.; Liao, D. Z.; Yan, S. P.; Jiang, Z. H. *J. Am. Chem. Soc.* **2004**, *126*, 15394. (d) Mahata, P.; Sankar, G.; Madras, G.; Natarajan, S. *Chem. Commun.* **2005**, 5787. (e) Zaleski, C. M.; Depperman, E. C.; Kampf, J. W.; Kirk, M. L.; Pecoraro, V. L. *Angew. Chem., Int. Ed.* **2004**, *43*, 3912. (f) Yue, Q.; Yang, J.; Li, G. H.; Li, G. D.; Xu, W.; Chen, J. S.; Wang, S. N. *Inorg. Chem.* **2005**, *44*, 5241.
- (9) (a) Zhang, M. B.; Zhang, J.; Zheng, S. T.; Yang, G. Y. *Angew. Chem., Int. Ed.* **2005**, *44*, 1385. (b) Cheng, J. W.; Zhang, J.; Zheng, S. T.; Zhang, M. B.; Yang, G. Y. *Angew. Chem., Int. Ed.* **2006**, *45*, 73.

- (10) (a) Sheldrick, G. M. *SHELXS97. A Program for the Solution of Crystal Structures from X-ray Data*; University of Göttingen: Göttingen, Germany, 1997. (b) Sheldrick, G. M. *SHELXL97. A Program for the Refinement of Crystal Structures from X-ray Data*; University of Göttingen: Göttingen, Germany, 1997.

Table 2. Selected Bond Lengths (Å) and Angles (deg) for Compounds **1** and **2**^a

Compound 1			
Nd1–O3	2.414(3)	Nd1–O4	2.507(3)
Nd1–O1 ^{#1}	2.362(3)	Nd1–O2 ^{#4}	2.510(3)
Ag1–N1	2.309(4)	Ag1–O4	2.327(3)
O1 ^{#1} –Nd1–O1 ^{#2}	161.87(18)	O3–Nd1–O1 ^{#1}	82.33(12)
O4–Nd1–O1 ^{#2}	124.28(12)	O3–Nd1–O4	132.61(11)
O4–Nd1–O2 ^{#4}	72.64(12)	O3–Nd1–O3 ^{#3}	73.83(18)
O4–Nd2–O4 ^{#3}	51.17(15)	O3 ^{#3} –Nd1–O2 ^{#4}	145.71(13)
N1–Ag1–N1 ^{#5}	102.8(2)	N1–Ag1–O4	112.38(15)
O4–Ag1–O4 ^{#5}	118.55(17)	O4–Ag1–N1 ^{#5}	104.90(14)
Compound 2			
Eu1–O3	2.372(3)	Eu1–O4	2.475(3)
Eu1–O2 ^{#1}	2.318(3)	Eu1–O1 ^{#4}	2.462(3)
Ag1–N1	2.311(4)	Ag1–O4	2.319(3)
O2 ^{#1} –Eu1–O2 ^{#2}	162.34(16)	O3–Eu1–O2 ^{#1}	82.45(11)
O4–Eu1–O2 ^{#2}	124.45(12)	O3–Eu1–O4	132.51(11)
O4–Eu1–O1 ^{#4}	72.77(11)	O3–Eu1–O3 ^{#3}	73.59(16)
O4–Eu2–O4 ^{#3}	51.96(14)	O3 ^{#3} –Nd1–O1 ^{#4}	145.47(12)
N1–Ag1–N1 ^{#5}	102.6(2)	N1–Ag1–O4	112.38(15)
O4–Ag1–O4 ^{#5}	118.06(16)	O4–Ag1–N1 ^{#5}	104.92(14)

^a Symmetry operations. For **1**: (#1) $x - y, x - 1, z + 1/6$; (#2) $-y + 2, -x + 3, -z - 1/6$; (#3) $x - y + 1, -y + 2, -z$; (#4) $-x + 3, -x + y + 2, -z - 1/3$; (#5) $-y + 2, -x + 2, -z - 1/6$. For **2**: (#1) $x - y, x, z + 1/6$; (#2) $-x + y + 2, y + 1, -z + 1/2$; (#3) $-x + 2, -x + y + 1, -z + 2/3$; (#4) $y + 1, x, -z + 1/3$; (#5) $-x + y + 1, y, -z + 1/2$.

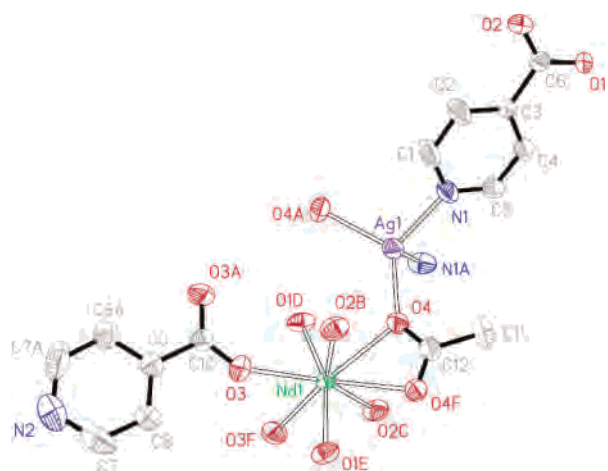


Figure 1. ORTEP plot of the asymmetric unit of **1** (50% probability ellipsoids). All H atoms are omitted for clarity. Symmetry codes: A ($-y + 2, -x + 3, -z - 1/6$); B ($-x + 3, -x + y + 2, -z - 1/3$); C ($-y + 2, x - y, z + 1/3$); D ($x - y, x - 1, z + 1/6$); E ($-y + 2, -x + 3, -z - 1/6$); F ($x - y + 1, -y + 2, -z$).

one OAc ligand, four O atoms from four bridging IN ligands, and two O atoms from two terminal IN ligands. The Nd–O bond lengths [2.362(3)–2.510(3) Å] are in the normal range.¹¹ IN ligands have two types of distinctly different coordination modes: one acts as a bridging ligand to coordinate one Ag(I) ion and two Nd(III) ions (Chart 1a) and the other acts as a terminal ligand to coordinate two Nd(III) ions (Chart 1b). OAc adopts chelating and bridging coordination modes (Chart 1c). In the structure of **1**, the chiral unit can be considered as a right-handed inorganic heterometallic helical chain built up from the alternate Nd(III) and Ag(I) coordination centers with shared carboxylate O atoms (Figure 2). The 6_1 screw axis passes down the center of the

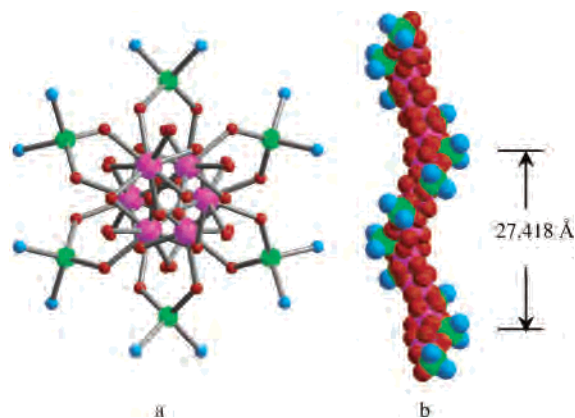
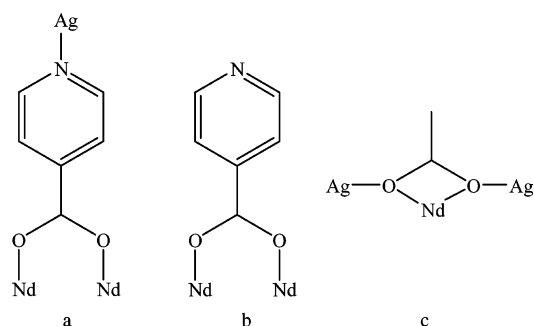


Figure 2. Right-handed heterometallic helicate with Nd–O–Ag connectivity: a ball-and-stick representation along the c axis (a) and a space-filling representation along the b axis (b). Color code: pink, Nd; green, Ag; red, O; blue, N. C and H atoms are omitted for clarity.

Chart 1. Coordination Modes of IN and OAc in **1**



helical chain with a pitch of 27.418 Å. It is noteworthy that the helical chains with Ln–O–M connectivity are quite rare. Up to now, to our knowledge, only two homochiral helical chains with Ln–O–Cu connectivity have been reported.^{8a}

Compared to homometal lanthanide coordination polymers containing IN ligands, in which the N donor atoms are free,¹² Ln–M–IN heterometallic coordination frameworks are built up from the nanosized lanthanide clusters and transition-metal clusters through the recognition between two types of metal ions and multifunctional ligands.⁹ In the structure of **1**, a homochiral helical chain forms by introducing the second ligand, OAc, and a soft transition-metal ion, Ag(I). OAc ligands connect to two types of metal centers in both chelating and bridging modes along different directions, which, therefore, lead to a noncentrosymmetric organization and a twist of the chain and the helical structure finally forms (Figure S2 in the Supporting Information). Furthermore, the lack of a symmetry center of two types of metal centers also ensures the acentricity of the chain and provides the possibility constructing a homochiral helical chain. On the other hand, the Ag(I) ion with a noncentrosymmetric coordination geometry also plays an important role in the formation of helical chains. In the current work, the occurrence of the helical structure of **1** may be attributed to the inducement of the Ag(I) ion¹³ and the coordination mode of

(11) Vaidhyanathan, R.; Natarajan, S.; Rao, C. N. R. *Inorg. Chem.* **2002**, *41*, 4496.

(12) Ma, L.; Evans, O. R.; Foxman, B. M.; Lin, W. *Inorg. Chem.* **1999**, *38*, 5837.

(13) (a) Prince, R. B.; Okada, T.; Moore, J. S. *Angew. Chem., Int. Ed.* **1999**, *38*, 233. (b) Chen, X. D.; Du, M.; Mak, T. C. *Chem. Commun.* **2005**, 4417.

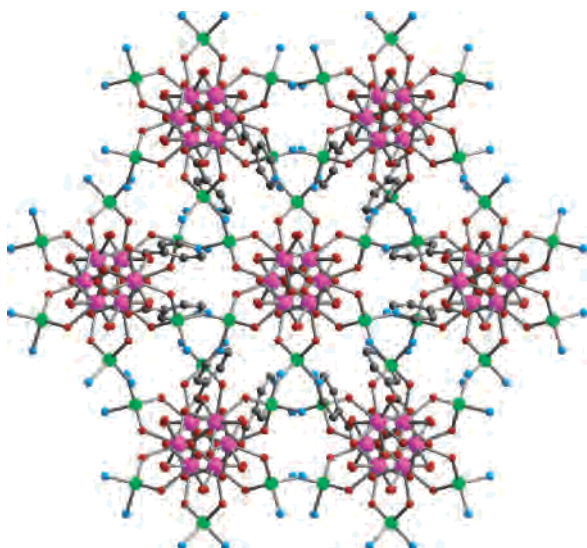


Figure 3. Perspective view of the 3D coordination framework in **1** along the *c* axis.

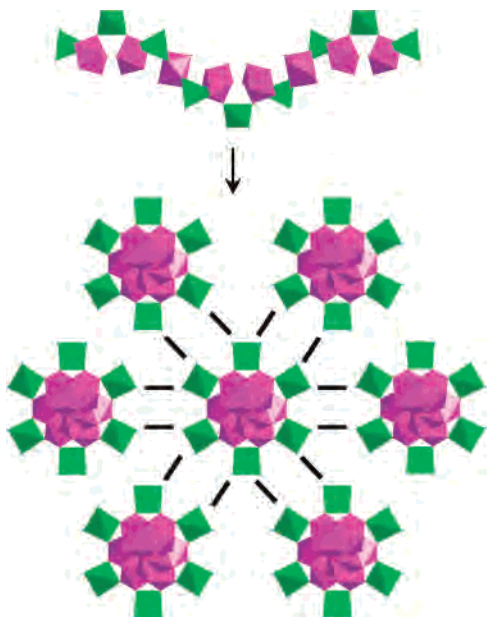


Figure 4. Polyhedral view of a helical chain interleaved with six other neighboring chains in **1**. The bold line represents the IN ligand.

OAc.¹⁴ It is interesting that the helical chains in **1** are not polar because of the 2-fold rotation axis going through the Ag(I) and Nd(III) centers.

The distinguishing feature of **1** is that the helical chains are connected together by IN spacers to form a homochiral 3D framework, as shown in Figure 3. Terminal IN ligands are around the helical chains and toward the space constructed by the stacking of the helical chains. Figure 4 shows an expanded view of the packing around one helical chain. One helical chain is interleaved by six more helices with the same handedness, which ensures acentric helix packing

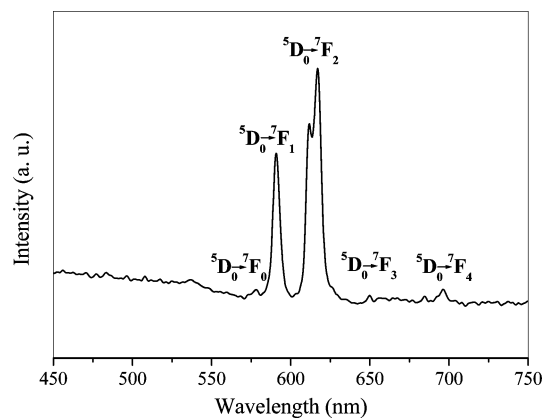


Figure 5. Solid-state emission spectrum for **2** at room temperature (excited at 396 nm).

without introduction of an inversion center between them. It is well-known that helical structural motifs exhibit an axial chirality,¹⁵ and packing these 1D helical chains into a homochiral solid needs homochiral discriminative interactions. In the structure of **1**, the coordination bonds between IN ligands and two types of metal centers offer the homochiral interactions to realize the homochiral assembly. In other words, spontaneous resolution yielding homochiral crystals occurs in **1** through interchain coordination bonds that chemically assemble these right-handed helices. Furthermore, the observed chirality of **1**, indicated by its hexagonal chiral space group, can be understood in terms of chirality transfer from the chiral helical chains to the whole framework through the coordination bonds between IN ligands and two types of metal centers.

TGA. A TGA study of **1** shows no weight loss between room temperature and 290 °C, suggesting that the framework is stable up to 290 °C (Figure S5 in the Supporting Information). Such a thermal stability of **1** may be attributed to the formation of a 1D heterometallic helical chain with Ln–O–Ag connectivity. Above 290 °C, the weight loss is due to the collapse of the whole framework. The result of the TGA study for **2** (Figure S6 in the Supporting Information) is very similar.

Photoluminescent Properties. Because of the excellent luminescent properties of Eu(III) ions, the luminescence of **2** was investigated. The emission spectrum of **2** (see Figure 5) at room temperature upon excitation at 396 nm displays red luminescence and exhibits the characteristic transition of $^5D_0 \rightarrow ^7F_J$ ($J = 0-4$) of Eu(III) ions. The appearance of the symmetry-forbidden emission $^5D_0 \rightarrow ^7F_0$ at 580 nm indicates that Eu(III) ions in **2** possess the noncentrosymmetric coordination environment.^{8c} It is known that the $^5D_0 \rightarrow ^7F_1$ transition is a magnetic dipole transition, and its intensity varies with the crystal-field strength acting on the Eu(III) ion. The $^5D_0 \rightarrow ^7F_2$ transition is an electric dipole transition and is extremely sensitive to the coordination environment of the Eu(III) ion. The intensity of the $^5D_0 \rightarrow ^7F_2$ transition increases as the site symmetry of the Eu(III) center decreases. In the spectrum of **2**, the strongest emission

(14) (a) Yu, Z. T.; Liao, Z. L.; Jiang, Y. S.; Li, G. H.; Li, G. D.; Chen, J. S. *Chem. Commun.* **2004**, 1814. (b) Milios, C. J.; Kefalloniti, E.; Raptopoulou, C. P.; Terzis, A.; Vicente, R.; Lalioti, N.; Escuer, A.; Perlepes, S. P. *Chem. Commun.* **2003**, 819. (c) Tasiopoulos, A. J.; Harden, N. C.; Abboud, K. A.; Christou, G. *Polyhedron* **2003**, *22*, 133.

(15) Piguet, C.; Bernardinelli, G.; Hopfgartner, G. *Chem. Rev.* **1997**, *97*, 2005.

peak in the $^5D_0 \rightarrow ^7F_2$ transition region is split into two levels at 612 and 617 nm, which can be ascribed to the splitting of energy levels. Because Eu(III) centers in **2** possess a C_1 -symmetric coordination environment, in principle, the emission peak in the $^5D_0 \rightarrow ^7F_2$ transition can be split into five peaks. In the present work, because of some important factors such as the short decay lifetime of lanthanide ions and the superposition of emission peaks, only two of these peaks appear in the current emission spectrum. The intensity of the $^5D_0 \rightarrow ^7F_1$ transition is the second strongest, and the emission peak centers at 590 nm. The intensity ratio $I(^5D_0 \rightarrow ^7F_2)/I(^5D_0 \rightarrow ^7F_1)$ is equal to ca. 1.5, which further confirms that Eu(III) ions in **2** occupy sites with low symmetry and without an inversion center.¹⁶ The red emission of the $^5D_0 \rightarrow ^7F_2$ transition is the most intense, suggesting that the achiral ligands are suitable for the sensitization of red luminescence for the Eu(III) ion.¹⁷ As to the IN ligand, the luminescence emission spectrum is shown in Figure S7 in the Supporting Information. The absence of the ligand-based emission in the spectrum of **2** also suggests that the energy transfer from the ligand to the Eu(III) center is effective.

(16) Bünzli, J.-C. G. In *Lanthanide Probes in life, Chemical and Earth Sciences. Theory and Practice*; Bünzli, J.-C. G., Choppin, G. R., Eds.; Elsevier Scientific Publishers: Amsterdam, The Netherlands, 1989; Chapter 7.

(17) De Betterncourt Dias, A.; Viswanathan, S. *Chem. Commun.* **2004**, 1024.

Conclusions

In conclusion, we have successfully synthesized two homochiral 3D Ln–Ag heterometallic coordination polymers. These two complexes are isostructural, and their frameworks are constructed from the infinite right-handed chains with Ln–O–Ag connectivity. They represent the first examples of a 3D homochiral Ln–M heterometallic coordination framework assembled by a right-handed inorganic helical chain based on spontaneous resolution. The successful synthesis of both compounds not only provides novel examples of homochiral 3D Ln–M heterometallic coordination framework but also may promise a new strategy for the design of novel homochiral 3D Ln–M heterometallic coordination polymer materials with particular functions.

Acknowledgment. This work was financially supported by a Program for New Century Excellent Talents in University (Grant NCET-05-0278), the National Natural Science Foundation of China (Grant 20471012), and the Foundation for the Author of National Excellent Doctoral Dissertation of China (Grant 200322).

Supporting Information Available: X-ray crystallographic files for **1** and **2** in CIF format, additional figures, IR spectra, TGA curves, and photoluminescence spectra. This material is available free of charge via the Internet at <http://pubs.acs.org>.

IC060806L